

Supplementary material

Turn-on fluorescent probe toward glyphosate and Cr³⁺ based on Cd(II)-metal organic framework with Lewis basic sites

Theanchai Wiwasuku,^a Jaursup Boonmak,^{a*} Rodjana Burakam,^a Sarinya Hadsadee,^b Siriporn Jungsuttiwong,^b Sareeya Bureekaew,^c Vinich Promarak,^d and Sujitra Youngme^a

^aMaterials Chemistry Research Centre, Department of Chemistry and Centre of Excellence for Innovation in Chemistry, Faculty of Science, Khon Kaen University, Khon Kaen, 40002, Thailand.

^bCenter for Organic Electronic and Alternative Energy, Department of Chemistry and Center of Excellence for Innovation in Chemistry, Faculty of Science, Ubon Ratchathani University, Ubon Ratchathani 34190, Thailand

^cSchool of Energy Science and Engineering, Vidyasirimedhi Institute of Science and Technology (VISTEC), Rayong , 21210, Thailand.

^dSchool of Molecular Science and Engineering, Vidyasirimedhi Institute of Science and Technology (VISTEC), Rayong , 21210, Thailand.

*E-mail: jaursup@kku.ac.th

Parameter	1	1-NH₂
Empirical formula	C ₁₈ H ₁₂ CdN ₄ O ₄	C ₁₈ H ₁₃ CdN ₅ O ₄
Formula weight	460.72	475.73
Crystal system	Orthorhombic	Orthorhombic
Space group	<i>Cmca</i>	<i>Cmca</i>
a (Å)	13.6401(5)	13.7017(6)
b (Å)	20.7509(7)	20.9274(8)
c (Å)	14.4681(5)	14.7410(7)
α (°)	90	90
β (°)	90	90
γ (°)	90	90
V (Å ³)	4095.1(2)	4226.8(3)
Z	8	8
D _{calc} (gcm ⁻³)	1.495	1.495
Data/res/parameters	2538/173/151	2258/183/157
GOF on F ²	0.794	0.902
R ₁ ^a , wR ₂ ^b [I > 2α(I)]	0.0375/0.1063	0.0.0449/0.1419
R ₁ ^a , wR ₂ ^b (all data)	0.0448/0.1117	0.0614/0.1518

Table S1 Crystallographic data and structural refinement for **1** and **1-NH₂**

$$^a R_1 = \sum \|F_0\| - \|F_c\| / \sum \|F_0\|, \quad ^b wR_2 = [\sum w(F_o^2 - F_c^2)^2 / \sum w(F_o^2)]^{1/2}$$

Table S2 Selected bond distances (\AA) and angle ($^\circ$) for compound **1**

	Distances (\AA)
Cd1—O2	2.300(3)
Cd1—N1	2.320(3)
Cd1—N1 ¹	2.320(3)
Cd1—O1 ²	2.346(4)
Cd1—O4 ³	2.365(3)
Cd1—O3 ³	2.393(3)
Cd1—O3 ³	2.607(3)
	Angles ($^\circ$)
O2—Cd1—N1	92.97(9)
O2—Cd1—N1 ¹	92.97(9)
N1—Cd1—N1 ¹	170.43(17)
O2—Cd1—O1 ²	130.10(11)
N1—Cd1—O1 ²	85.22(8)
N1 ¹ —Cd1—O1 ²	85.21(8)
O2—Cd1—O4 ³	84.71(12)
N1—Cd1—O4 ³	94.01(8)
N1 ¹ —Cd1—O4 ³	94.01(8)
O1 ² —Cd1—O4 ³	145.18(11)
O2—Cd1—O3 ³	139.75(11)
N1—Cd1—O3 ³	90.16(8)
N1 ¹ —Cd1—O3 ³	90.15(8)
O1 ² —Cd1—O3 ³	90.15(10)
O4 ³ —Cd1—O3 ³	55.03(11)
O2—Cd1—O1	52.76(11)
N1—Cd1—O1	88.81(8)
N1 ¹ —Cd1—O1	88.81(8)
O1 ² —Cd1—O1	77.34(12)
O4 ³ —Cd1—O1	137.47(11)
O3 ³ —Cd1—O1	167.49(11)

Symmetry codes: (1) $I-x$, $+y$, $+z$; (2) $I-x$, $I-y$, $I-z$; (3) $+x$, $-I/2+y$, $I/2-z$; (4) $+x$, $I/2+y$, $I/2-z$

Table S3 Selected bond distances (\AA) and angle ($^\circ$) for compound **1-NH₂**

	Distances (\AA)
Cd1—O1	2.242(5)
Cd1—O2 ¹	2.326(6)
Cd1—O4 ²	2.327(5)
Cd1—N1 ³	2.340(5)
Cd1—N1	2.340(5)
Cd1—O3 ²	2.423(5)
	Angles ($^\circ$)
O1—Cd1—O2 ¹	128.61(18)
O1—Cd1—O4 ²	142.39(18)
O2 ¹ —Cd1—O4 ²	89.00(16)
O1—Cd1—N1 ³	91.69(11)
O2 ¹ —Cd1—N1 ³	85.73(11)
O4 ² —Cd1—N1 ³	91.17(10)
O1—Cd1—N1	91.69(11)
O2 ¹ —Cd1—N1	85.73(11)
O4 ² —Cd1—N1	91.17(10)
N1 ³ —Cd1—N1	171.1(2)
O1—Cd1—O3 ²	88.19(18)
O2 ¹ —Cd1—O3 ²	143.20(17)
O4 ² —Cd1—O3 ²	54.20(17)
N1 ³ —Cd1—O3 ²	94.16(11)
N1—Cd1—O3 ²	94.16(11)

Symmetry codes: (1) $I-x$, $-y$, $I-z$; (2) $+x$, $-I/2+y$, $I/2-z$; (3) $I-x$, $+y$, $+z$; (4) $+x$, $I/2+y$, $I/2-z$

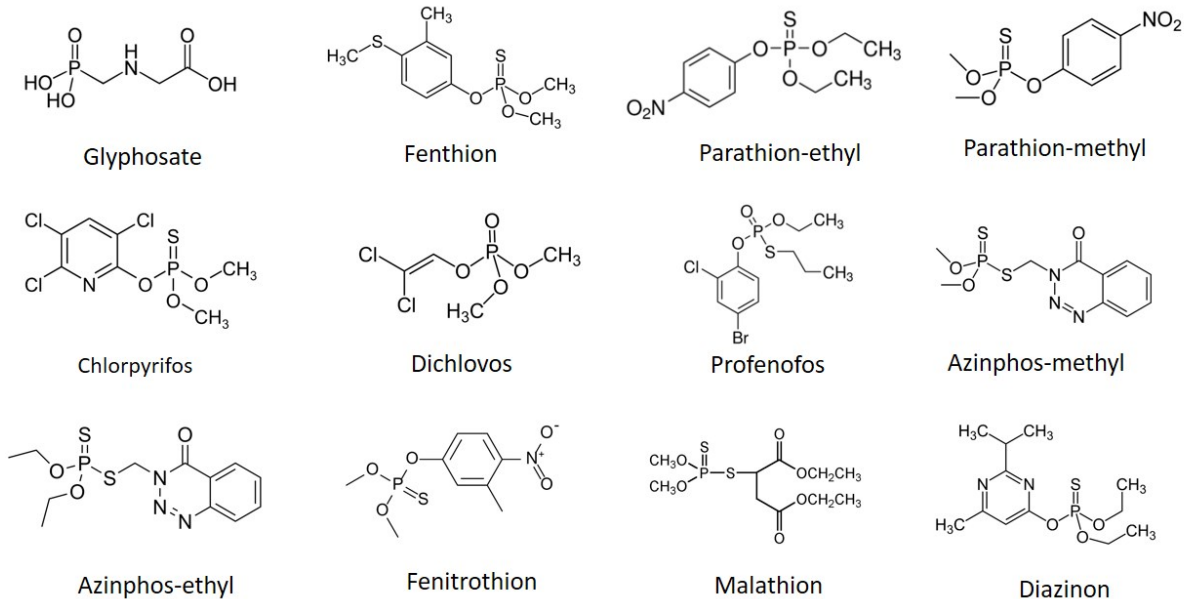


Fig. S1 Chemical structures of the selected pesticides.

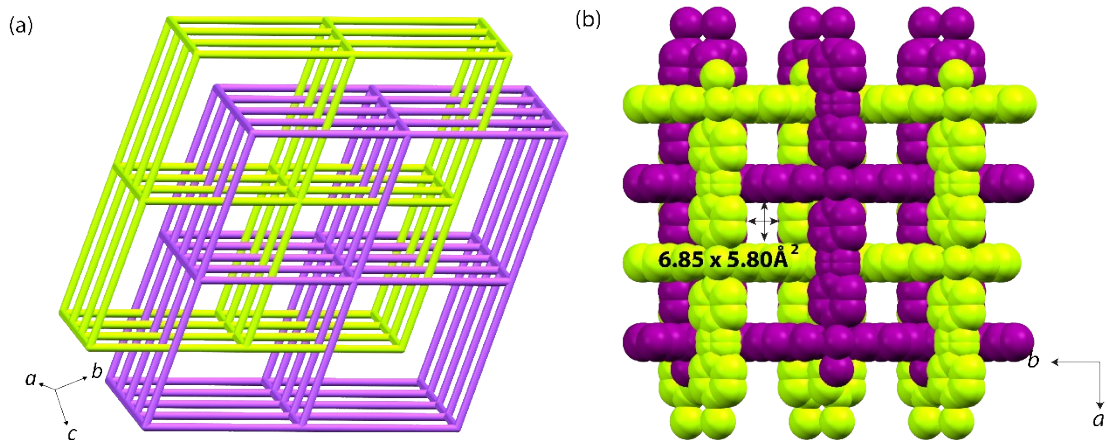


Fig. S2 (a) Topological feature of **1-NH₂** along *a* axis. (b) 2-fold interpenetrated 3D framework

of **1-NH₂** in space filling mode.

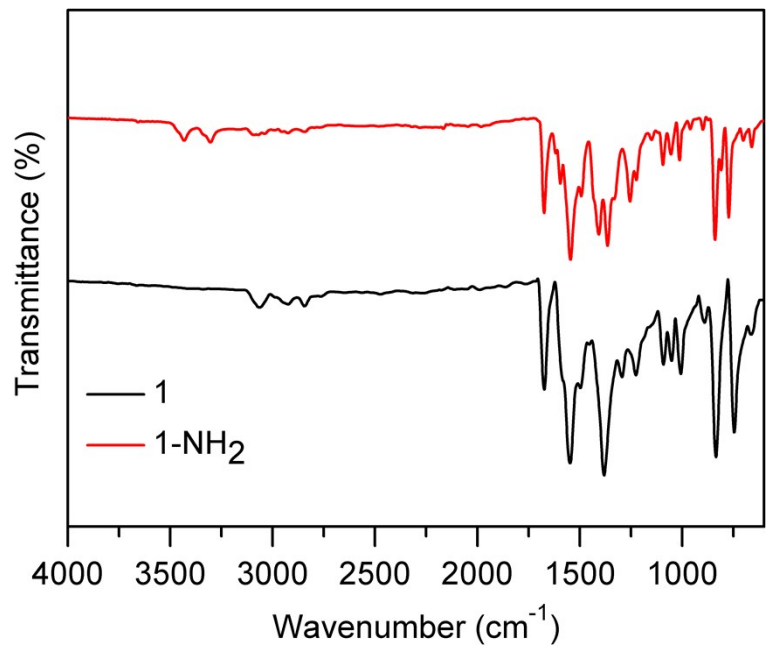


Fig. S3 FT-IR spectra of **1** and **1-NH₂**.

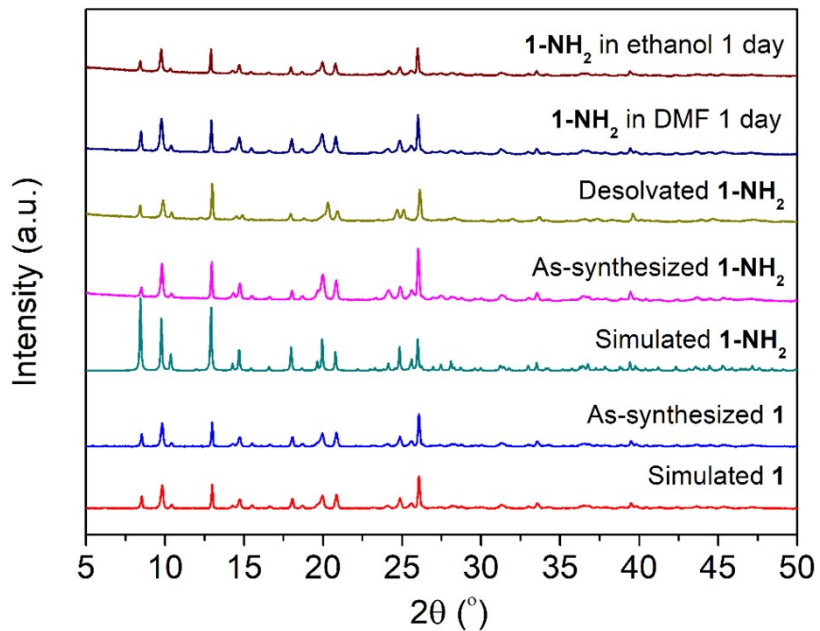


Fig. S4 PXRD patterns for the simulated and as-synthesized **1** and **1-NH₂**.

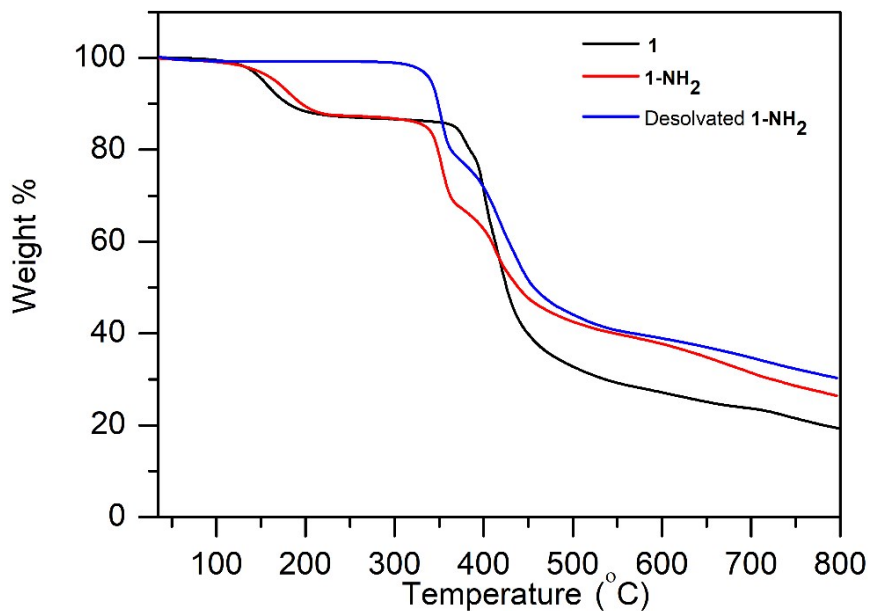


Fig. S5 TGA curves for as-synthesized **1** and **1-NH₂** and desolvated **1-NH₂**.

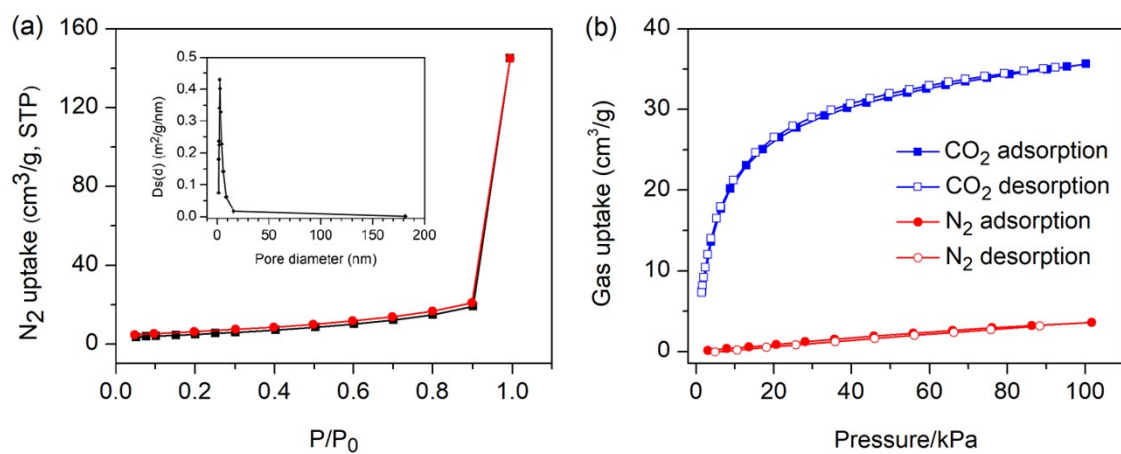


Fig. S6 (a) N₂ adsorption isotherm of desolvated **1-NH₂** at 77 K (inset: pore size distribution of desolvated **1-NH₂**) (b) Gas adsorption isotherms of desolvated **1-NH₂** at 295 K.

Table S4 Calculation of standard deviation of fluorescence intensity for glyphosate sensing

Blank reading (only 1-NH₂)	Fluorescent intensity at 434 nm
Reading 1	4437.849
Reading 2	4614.951
Reading 3	4526.954
Reading 4	4558.367
Reading 5	4460.107
Reading 6	4387.441
Reading 7	4377.512
Reading 8	4462.322
Reading 9	4533.827
Reading 10	4670.202
Standard deviation (δ)	95.4051
Slope from calibration graph (m)	11375.0506
LOD (3δ/m)	0.025 μ M

Table S5 Fluorescent sensor for glyphosate detection based on MOF and other fluorescent materials

Fluorescent material	Fluorescent response	Mechanism	LOD	Ref.
MOFs				
Fe ₃ O ₄ @SiO ₂ @UiO-67	Enhancement	Electron transfer	1 μM	[1]
[Cd(NH ₂ -bdc)(azp)]·DMF	Enhancement	Structural dissociation inhibited PET	25 nM	This work
Other fluorescent materials				
IgG-Carbon dot	Enhancement	Immune Reaction	47 nM	[2]
Carbon dot	Enhancement	Competitive affinity	95 nM	[3]
Carbon dot	Quenching	Fluorescent-resonance energy transfer	0.6 μM	[4]
Graphene quantum dots-silver nanoparticles	Quenching	Reduction of metal-enhanced fluorescence	53 nM	[5]
Calixarene-grafted Ruthenium(II)bipyridine Doped Silica NPs	Enhancement	Switch on FRET	0.79 μM	[6]

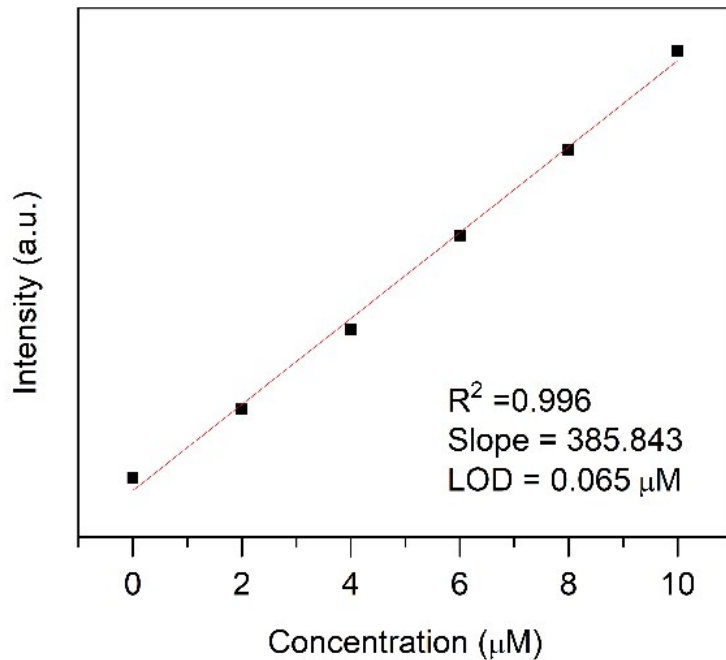


Fig. S7 The linear enhancement response of bulk phase **1-NH₂** toward glyphosate.

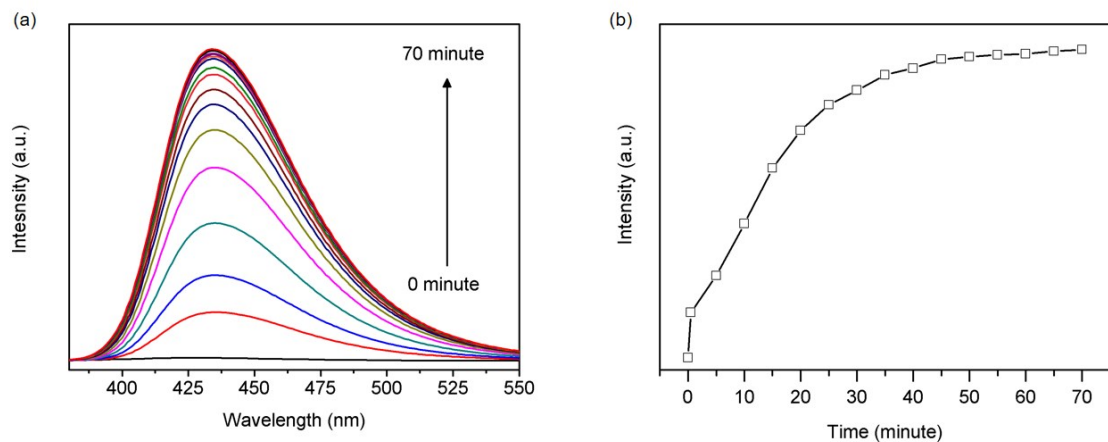


Fig. S8 (a) Fluorescence response of **1-NH₂** toward glyphosate at different times.

b) Plot of time dependent fluorescence intensity at 434 nm.

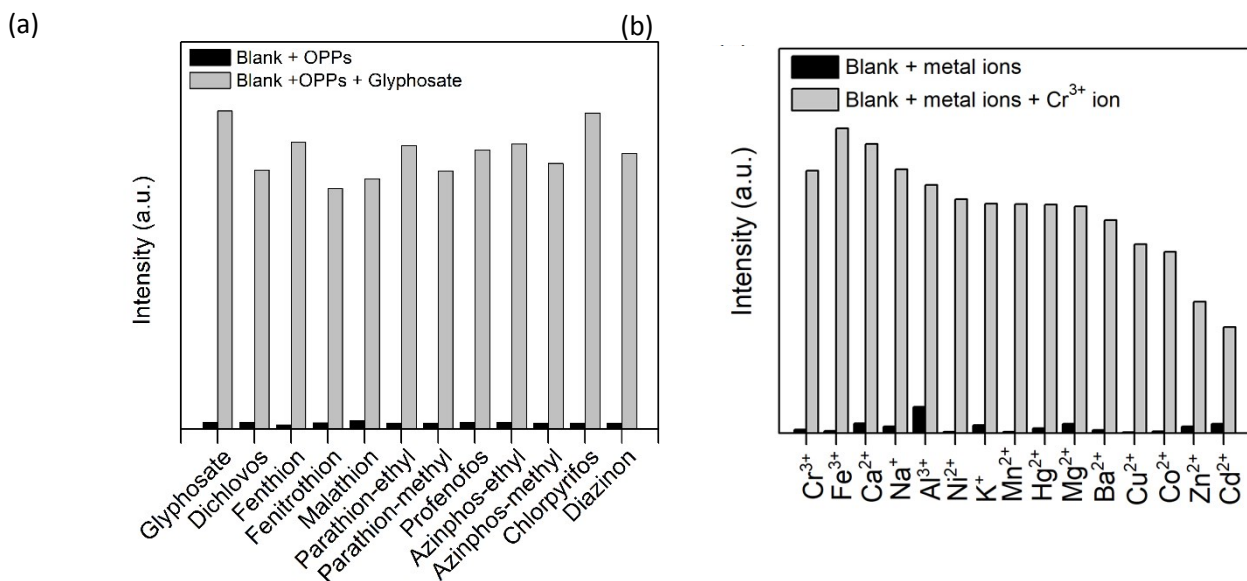


Fig. S9 (a) Fluorescent intensity response of **1-NH₂** at 434 nm in the presence of the selected OPPs (black bar) and **1-NH₂** + glyphosate upon the addition of interferent OPPs (gray bar) (total concentration of OPPs is 50 μ M). (b) Fluorescent intensity response of **1-NH₂** at 434 nm in the presence of the selected metal ions (black bar) and **1-NH₂** + Cr³⁺ upon the addition of interferent cations (gray bar) (total concentration of metal ions is 50 μ M).

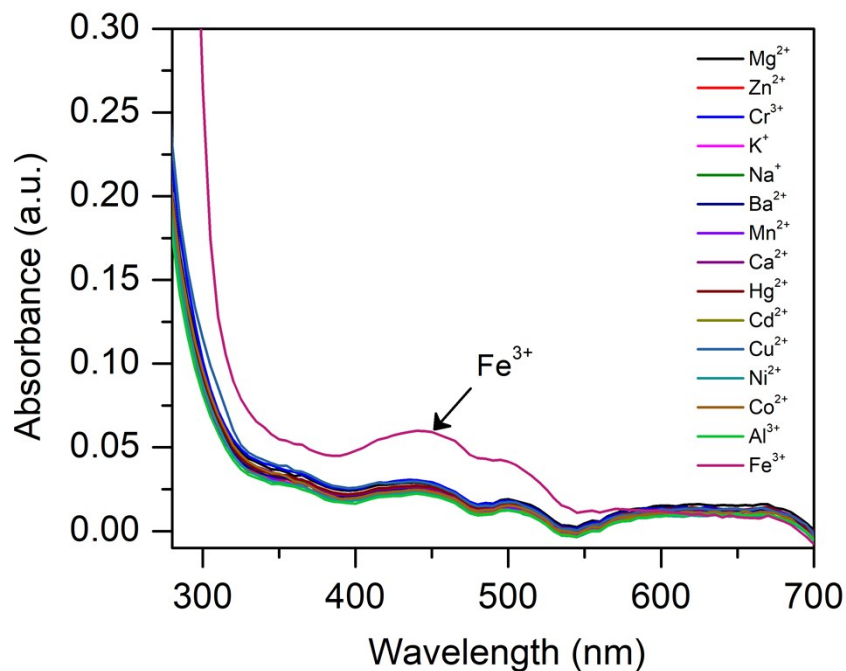


Fig. S10 UV-Vis absorption spectra of different metal ions in DMF.

Table S6 Calculation of standard deviation of fluorescence intensity for Cr^{3+} sensing

Blank reading (only $\mathbf{1-NH_2}$)	Fluorescent intensity at 434 nm
Reading 1	751.551
Reading 2	745.172
Reading 3	726.349
Reading 4	753.238
Reading 5	707.114
Reading 6	722.223
Reading 7	726.112
Reading 8	717.274
Reading 9	728.123
Reading 10	770.443
Standard deviation (δ)	19.4889
Slope from calibration graph (m)	98.7274
LOD (3δ/m)	0.60 μM

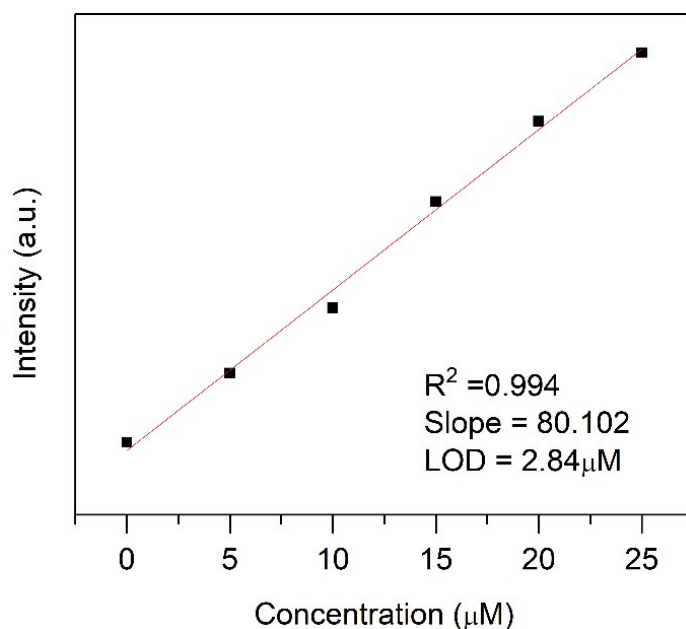


Fig. S11 The linear enhancement response of bulk phase $\mathbf{1-NH_2}$ toward Cr^{3+} .

Table S7 Fluorescent sensor for Cr³⁺ detection based on various MOFs and other fluorescent materials

Fluorescent material	Fluorescent response	Mechanism	LOD	Ref.
MOFs				
[Zn(L)(H ₂ O)]·H ₂ O	Quenching	Inner filter affect	2.44 μM	[7]
[Eu ₂ (tpbpc) ₄ ·CO ₃ ·H ₂ O]·DMF	Quenching	Inner filter affect & antenna effect inhibition	70 μM	[8]
[Zn ₂ (tpeb) ₂ (2,3-ndc) ₂]·H ₂ O	Quenching	Weak coordination	16 nM	[9]
Tb@[Cd ₄ (NDIC) ₄ (DMF) ₅ (H ₂ O)]·DMF	Quenching	Collapse of the structure	0.075 μM	[10]
[Zn ₃ (bpdc) ₂ (pdc) (DMF)]·6DMF	Quenching	Coordination inhibited energy transfer	25.1 μM	[11]
[Zn ₂ (TPOM)(NH ₂ -bdc) ₂]·4H ₂ O	Enhancement	Chelation enhanced fluorescence	4.9 μM	[12]
[Co ₃ (BIBT) ₃ (BTC) ₂ (H ₂ O) ₂]·solvents	Enhancement	Absorbance caused enhancement (ACE)	0.1 μM	[13]
[Cd(NH ₂ -bdc)(azp)]·DMF	Enhancement	Structural dissociation inhibited PET	0.6 μM	This work
Other fluorescent materials				
TGA-CdSe QDs	Quenching	Coordination modified valence band and conduction band energies	11.3 nM	[14]
RDC-1	Enhancement	Internal charge transfer	17.8 nM	[15]
Coumarin–Pyrazolone	Quenching	Nonfluorescent complex formation	37 pM	[16]
Gold nanoparticle	Enhancement	Aggregation induced emission	0.02 μM	[17]
PIN/CDS nanocomposite	Enhancement	Chelation enhanced fluorescence	0.47 μM	[18]

L = 5-(2-methylpyridin-4-yl)isophthalate; tpbpc = 4'-[4,2';6',4'"]-terpyridin-4'-yl-biphenyl-4-carboxylate; tpeb = 1,3,5-tri-4-pyridyl-1,2-ethenylbenzene; 2,3-ndc = 2,3-naphthalenedicarboxylic acid; NDIC = 5-(5-norbornene-2,3-dicarboximide)isophthalic acid; bpdc = 4,4'-biphenyldicarboxylic acid; pdc = pyridine-3,5-dicarboxylate, TPOM = tetrakis(4-pyridyloxymethylene)methane)

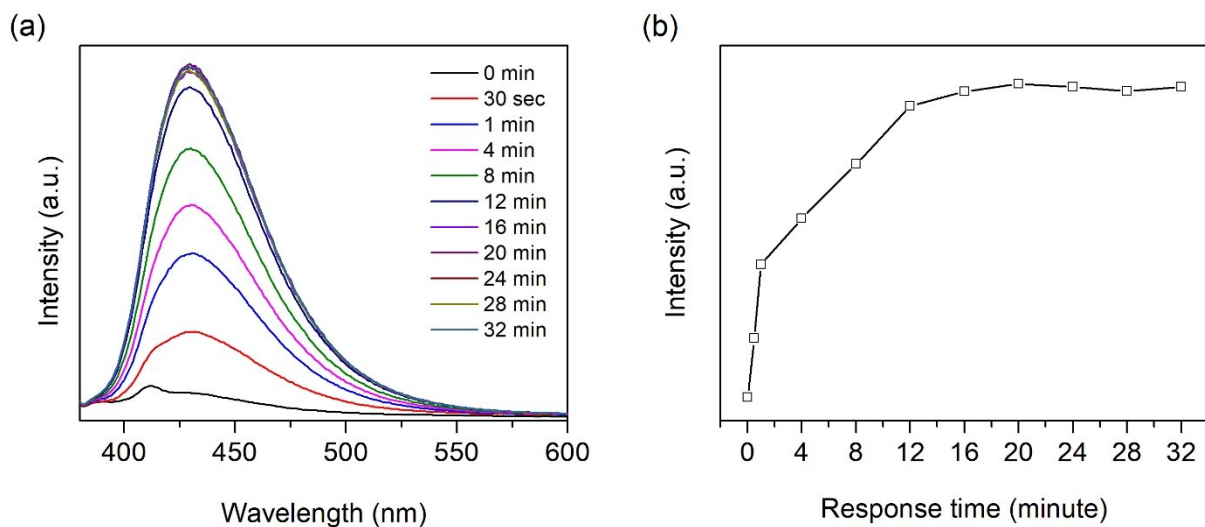


Fig. S12 (a) Fluorescence response of **1-NH₂** toward Cr³⁺ ion (20 μM) at 0-32 min.

(b) Plot of time dependent fluorescence intensity at 434 nm.

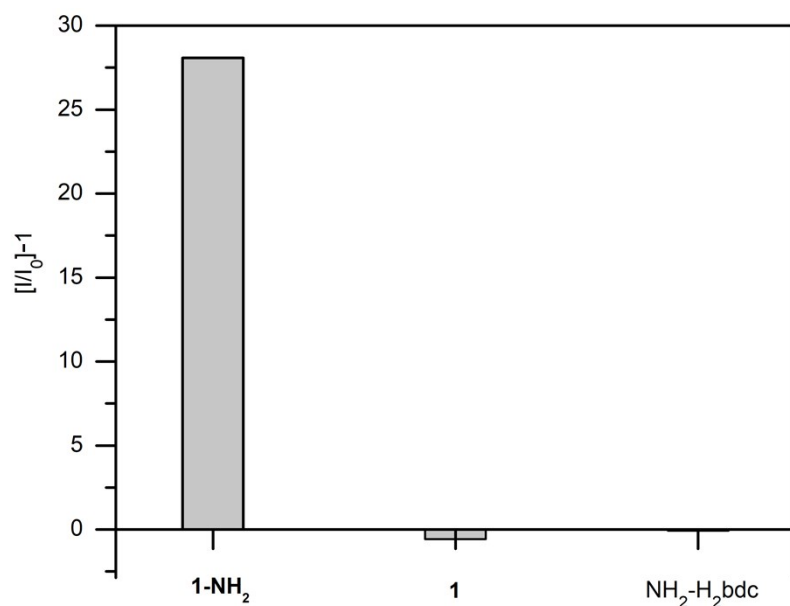


Fig. S13 The fluorescent response of **1-NH₂**, **1** and free NH₂-H₂bdc with the addition of 50 μM Cr³⁺ ion.

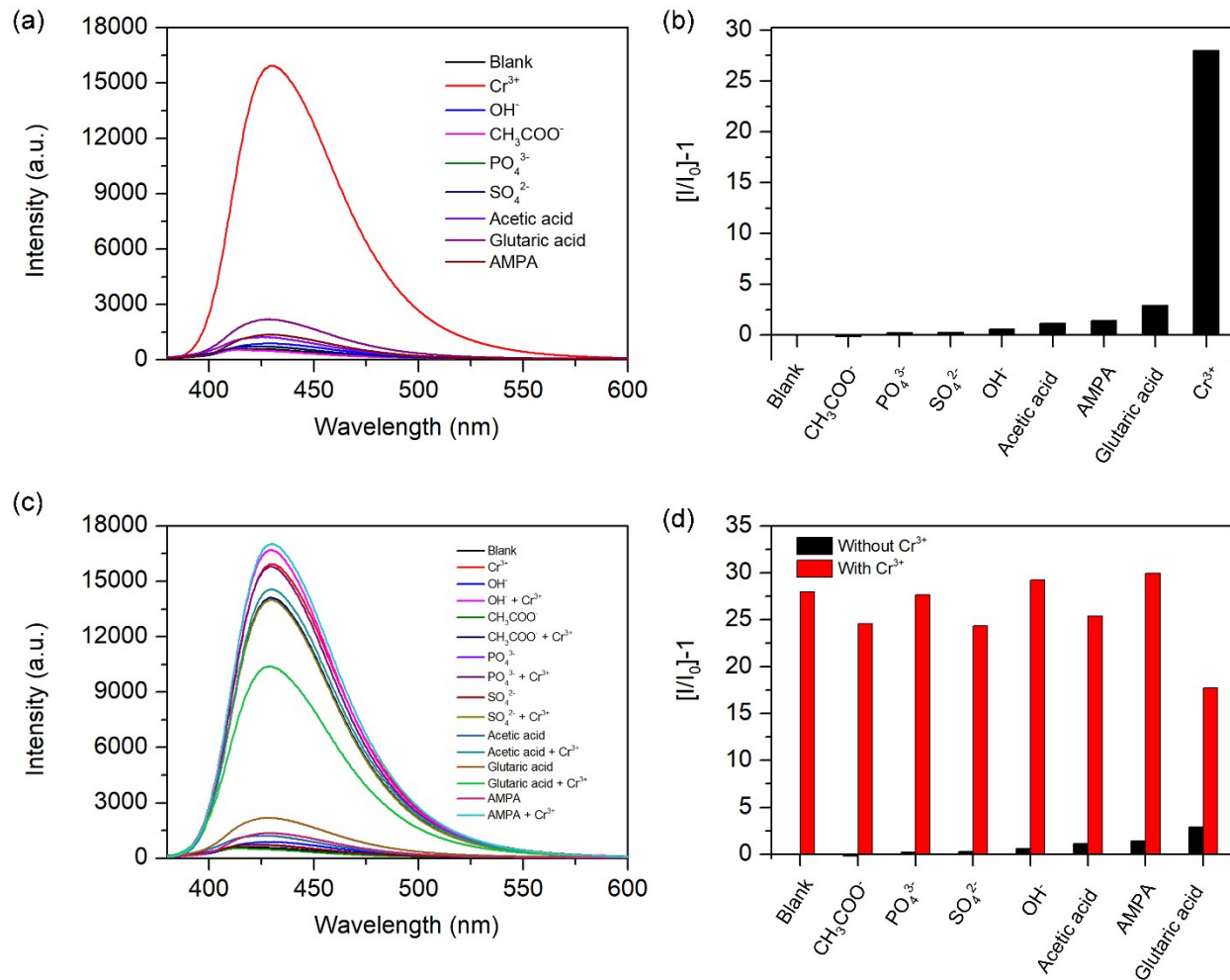


Fig. S14. (a) Fluorescent spectra and (b) fluorescent intensities of **1-NH₂** in the presence of 50 μM of different interfering species with respect to the emission at 434 nm in DMF media. (c) Fluorescent spectra and (d) fluorescent intensities of **1-NH₂** the presence of the interfering species without Cr³⁺ (black bar) and with Cr³⁺ (red bar).

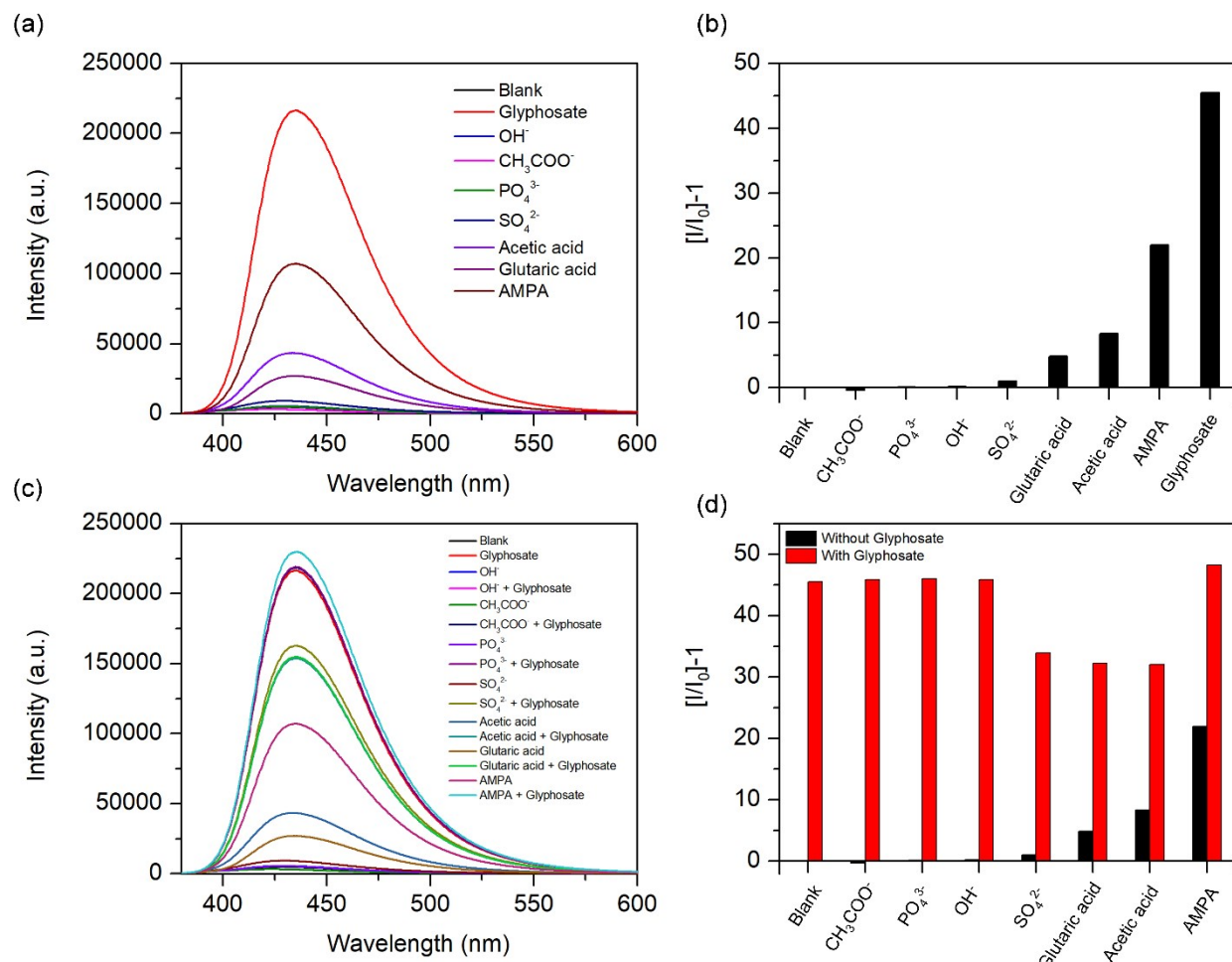


Fig. S15. (a) Fluorescent spectra and (b) fluorescent intensities of **1-NH₂** in the presence of 50 μM of different interfering species with respect to the emission at 434 nm in ethanol media. (c) Fluorescent spectra and (d) fluorescent intensities of **1-NH₂** the presence of the interfering species without glyphosate (black bar) and with glyphosate (red bar).

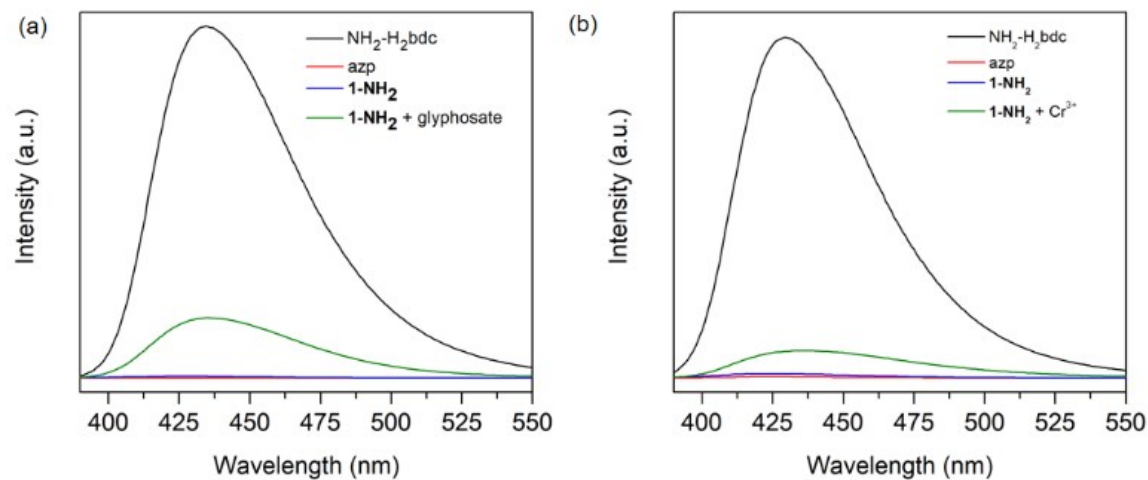


Fig. S16 Fluorescent emission of $\text{NH}_2\text{-H}_2\text{bdc}$, azp ligand, $\mathbf{1}\text{-NH}_2$, and $\mathbf{1}\text{-NH}_2 + \text{glyphosate}$ in ethanol media (a) and $\text{NH}_2\text{-H}_2\text{bdc}$, azp ligand, $\mathbf{1}\text{-NH}_2$, and $\mathbf{1}\text{-NH}_2 + \text{Cr}^{3+}$ in DMF.

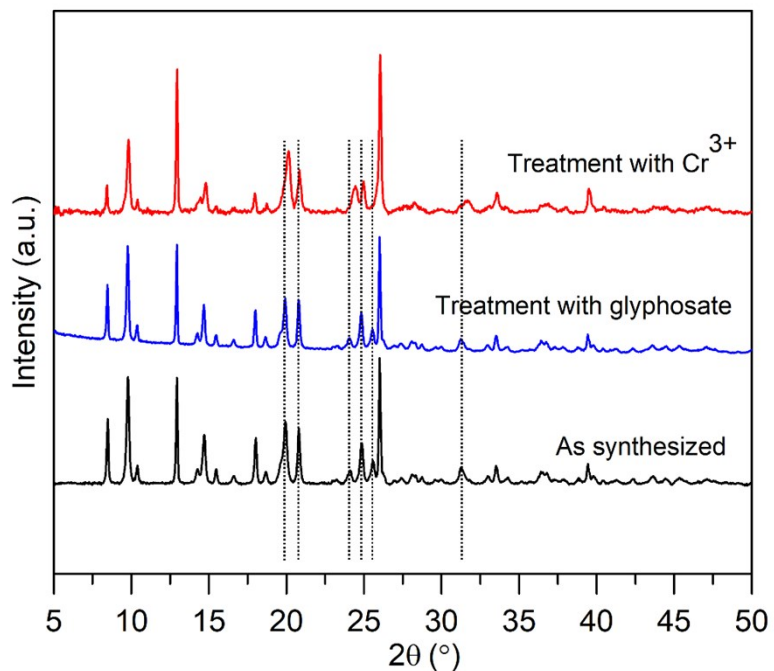


Fig. S17 PXRD patterns of as-synthesized and $\mathbf{1}\text{-NH}_2$ treated with Cr^{3+} for 1 day.

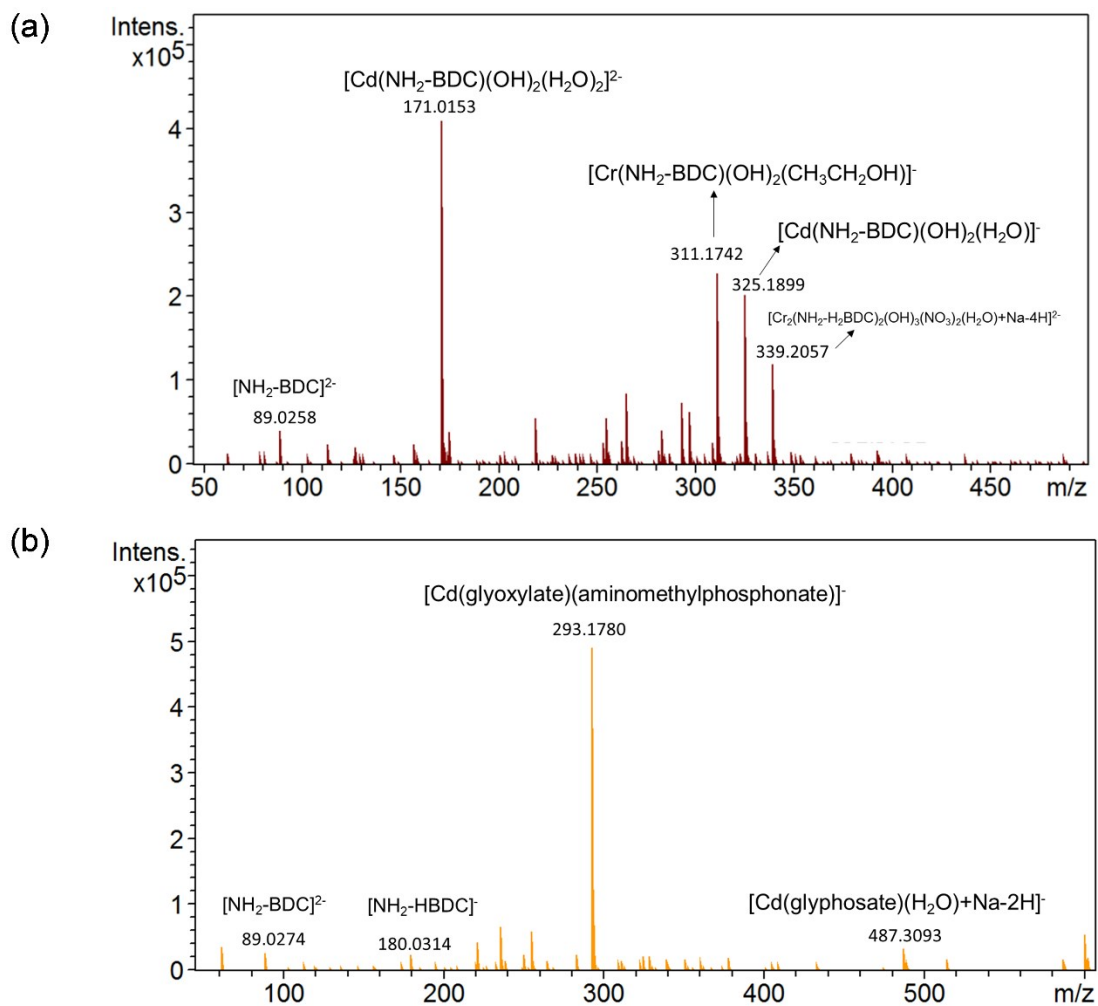


Fig. S18 ESI-MS spectra of **1-NH₂** upon the addition of (a) Cr³⁺ and (b) glyphosate.

References

- [1] Q. Yang, J. Wang, X. Chen, W. Yang, H. Pei, N. Hu, Z. Li, Y. Suo, T. Li and J. Wang, The simultaneous detection and removal of organophosphorus pesticides by a novel Zr-MOF based smart adsorbent. *J. Mater. Chem. A*, 2018, **6**, 2184–2192.
- [2] D. Wang, B. Lin, Y. Cao, M. Guo and Y. Yu, A highly selective and sensitive fluorescence detection method of glyphosate based on an immune reaction strategy of carbon dot labeled antibody and antigen magnetic beads. *J. Agric. Food Chem.*, 2016, **64**, 6042–6050.
- [3] L. Wang, Y. Bi, J. Gao, Y. Li, H. Ding and L. Ding, Carbon dots based turn-on fluorescent probes for the sensitive determination of glyphosate in environmental water samples. *RSC Adv.*, 2016, **6**, 85820–85828.

- [4] Y. Yuan, J. Jiang, S. Liu, J. Yang, H. Zhang, J. Yan and X. Hu, Fluorescent carbon dots for glyphosate determination based on fluorescence resonance energy transfer and logic gate operation. *Sens. Actuators B Chem.*, 2017, **242**, 545–553
- [5] J. Jiménez-López, E. Llorente-Martínez, P. Ortega-Barrales and A. Ruiz-Medina, Graphene quantum dots-silver nanoparticles as a novel sensitive and selective luminescence probe for the detection of glyphosate in food samples. *Talanta*, 2020, **207**, 120344.
- [6] B. C. M. A. Ashwin, C. Saravanan, T. Stalin, P. Muthu-Eswaran and S. Rajagopal, FRET-based solid-state luminescent glyphosate sensor using calixarene-grafted ruthenium(ii)bipyridine doped silica nanoparticles. *ChemPhysChem*, 2018, **19**, 2768–2775.
- [7] X.-Y. Guo, F. Zhao, J.-J. Liu, Z.-L. Liu, and Y.-Q. Wang, An ultrastable zinc(ii)-organic framework as a recyclable multiresponsive luminescent sensor for Cr(III), Cr(VI) and 4-nitrophenol in the aqueous phase with high selectivity and sensitivity. *J. Mater. Chem. A*, 2017, **5**, 20035–20043.
- [8] J. Liu, G. Ji, J. Xiao, and Z. Liu, Ultrastable 1D europium complex for simultaneous and quantitative sensing of Cr(III) and Cr(VI) ions in aqueous solution with high selectivity and sensitivity. *Inorg. Chem.*, 2017, **56**, 4197–4205.
- [9] T.-Y. Gu, M. Dai, D. J. Young, Z.-G. Ren, and J.-P. Lang, Luminescent Zn(II) coordination polymers for highly selective sensing of Cr(III) and Cr(VI) in water. *Inorg. Chem.*, 2017, **56**, 4668–4678.
- [10] Y. Wang, H. Yang, G. Cheng, Y. W, and S. Lin, A new Tb(II)-functionalized layer-like Cd-MOF as luminescent probe for highselectively sensing of Cr³⁺. *CrystEngComm*, 2017, **19**, 7270–7276.
- [11] X. Meng, M.-J. Wei, H.-N. Wang, H.-Y. Zang, and Z.-Y. Zhou, Multifunctional luminescent Zn(ii)-based metal-organic framework for high proton-conductivity and detection of Cr³⁺ ions in the presence of mixed metal ions. *Dalton Trans.*, 2018, **47**, 1383–1387.
- [12] R. Lv, J. Wang, Y. Zhang, H. Li, L. Yang, S. Liao, W. Gu and X. Liu, An amino-decorated dual-functional metal-organic framework for highly selective sensing of Cr(III) and Cr(VI) ions and detection of nitroaromatic explosives. *J. Mater. Chem. A*, 2016, **4**, 15494–15500.
- [13] X.-M. Tian, S.-L. Yao, C.-Q. Qiu, T.-F. Zheng, Y.-Q. Chen, H. Huang, J.-L. Chen, S.-L. Liu, and H.-R. Wen, Turn-On Luminescent Sensor toward Fe³⁺, Cr³⁺, and Al³⁺ Based on a Co(II) Metal-Organic Framework with Open Functional Sites. *Inorg. Chem.* 2020, **59**, 2803–2810.
- [14] G. C. de Souza, ÁL'den E.A. de Santana, P. A. da Silva, D. V. Freitas, M. Navarro, A. P. S. Paim and A. F. Lavorante, Employment of electrochemically synthesized TGA-CdSe quantum dots for Cr³⁺ determination in vitamin supplements. *Talanta*, 2015, **144**, 986 – 991.
- [15] O. Sunnapu, N. G. Kotla, B. Maddiboyina, G. S. Asthana, J. Shanmugapriya, K. Sekar, S. Singaravel and G. Sivaraman, Rhodamine based effective chemosensor for Chromium(III) and their application in live cell imaging. *Sens. Actuators B Chem.*, 2017, **246**, 761 – 768.
- [16] K. Saravana Mani, R. Rajamanikandan, G. Ravikumar, B. Vijaya Pandiyan, P. Kolandaivel, M. Ilanchelian and S. P. Rajendran, Highly sensitive coumarin-pyrazolone probe for the detection of Cr³⁺ and the application in living cells. *ACS Omega*, 2018, **3**, 17212–17219.
- [17] L. Wang, J. Liu, Z. Zhou, M. Xu and B. Wang, Convenient fluorescence detection of Cr(III) in aqueous solution based on the gold nanoparticle mediated release of the acridine orange probe. *Anal. Methods*, 2017, **9**, 1786–1791.
- [18] M. Faraz, A. Abbasi, F. K. Naqvi, N. Khare, R. Prasad, I. Barman and R. Pandey, Polyindole/cadmium sulphide nanocomposite based turn-on, multi-ion fluorescence sensor for detection of Cr³⁺, Fe³⁺, and Sn²⁺ ions. *Sens. Actuators B Chem.*, 2018, **269**, 195 – 202.